Supporting information for: Morphological Transitions During Melting of Small Cylindrical Aggregates

Chenyu Jin[†,‡] and Hans Riegler[*,]

†*Max Planck Institute of Colloids and Interfaces, Science Park Golm, 14476 Potsdam, Germany*

‡*Current address: Max Planck Institute of Dynamics and Self-Organisation, Am Faßberg 17, 37077 Göttingen, Germany*

E-mail: hans.riegler@mpikg.mpg.de

1.) The GT cylinder and the floating cylinder

For a floating cylinder eq. (6) reads as:

$$\frac{dG_{\mathrm{I}}^{\mathrm{cylinder}}}{dV_{\mathrm{l}}} = \frac{dG_{\mathrm{I}}(liquid)}{dV_{\mathrm{l}}} - \frac{2}{h}\gamma_{\mathrm{sv}} \tag{S1}$$

and thus:

$$\Delta T_m^{\mathrm{cylinder}} = \frac{1}{S_{\mathrm{m}}}\left[(\frac{dG_{\mathrm{I}}(liquid)}{dV_{\mathrm{l}}})_{\mathrm{max}} - \frac{2\gamma_{\mathrm{sv}}}{h}\right] \tag{S2}$$

For the special case of the GT approach (fig. 1(a)) all energy contributions from the interfaces of the solid and liquid with the substrates can be ignored ($\gamma_{\mathrm{s1}} = \gamma_{\mathrm{l1}}$ and $\gamma_{\mathrm{s2}} = \gamma_{\mathrm{l2}}$). In addition, because of assumption 2.) the liquid/vapor interface does not change during the phase transition. Therefore eq. (6) reads as:

$$\frac{dG_{\mathrm{I}}^{\mathrm{GT}}}{dV_{\mathrm{l}}} = \frac{d}{dV_{\mathrm{l}}}(\gamma_{\mathrm{ls}}A_{\mathrm{ls}}) = -\frac{\gamma_{\mathrm{ls}}}{r} \tag{S3}$$

and thus one recovers the GT behavior[1]:

$$\Delta T_{\mathrm{m}}^{\mathrm{GT}} = -\frac{\gamma_{\mathrm{ls}}}{S_m} \cdot \frac{1}{r_0} \tag{S4}$$

The GT approach often appears in a somewhat more general version:[S1–S6]

$$\Delta T_{\mathrm{m}}^{\mathrm{GT}}(shape) = -\frac{\gamma_{\mathrm{ls}}}{S_{\mathrm{m}}} \cdot \frac{\alpha}{r_0} \tag{S5}$$

Eq. (S5) parametrises the shape by α ($\alpha = 1$ for cylindrical shapes, $\alpha = 2$ for spherical geometries[S7]). This approach is only correct for a few simple configurations (e. g., freely suspended spheres or long cylinders. In the cylinder case, if energy contributions from the

[1]Please note that $dG_{\mathrm{I}}/dV_{\mathrm{l}} \propto -1/r$. Because of the minus-sign, the largest r (i. e., r_0) yields the largest $dG_{\mathrm{I}}/dV_{\mathrm{l}}$.

cylinder base planes can be neglected (fig. 1a) in the main text).

The Gibbs-Thomson-Herring (GTH) approach[S8,S9] is the extension of the GT model for anisotropic solid/liquid interfacial energies (asymmetric Wulff polyhedra) and may be applied to solid aggregates embedded in its infinite-size liquid melt. However, it is not applicable to small solid aggregates embedded in a *finite* size melt because it does *not* consider the impact of the capillary interface.

2.) Experimental data: Rouloid and bulged morphologies

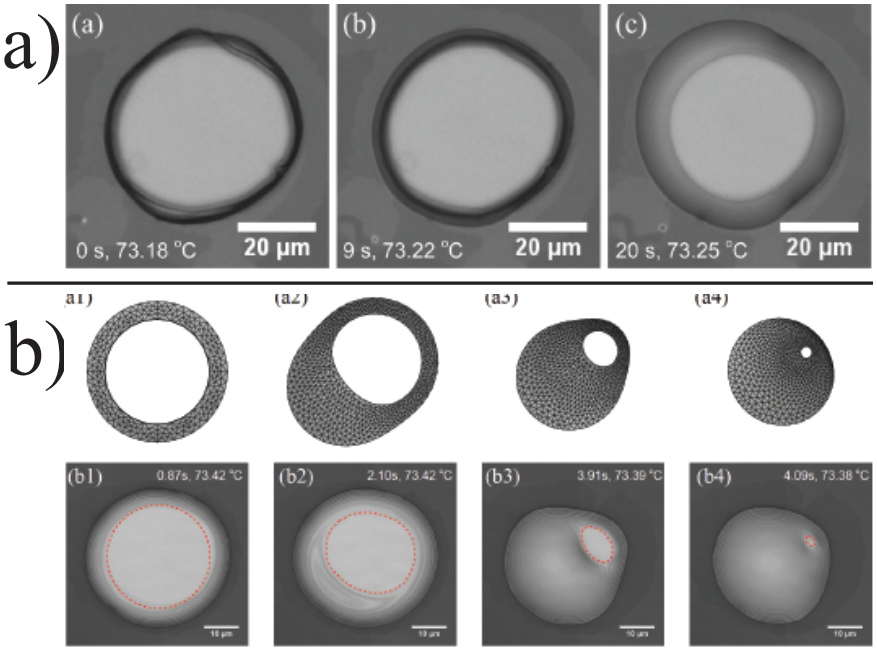

Figure S1: a) Evolution of a rouloid liquid channel morphology during a slight temperature increase (alkane islands: $C_{36}H_{74}$, $r_0 \approx 50\mu$m, $h \approx 2.2\mu$m, $\Theta \approx 20°$). b) Evolution of a bulged liquid channel morphology (top row: simulation, low row: experiments) under approximately isothermal conditions (alkane islands: $C_{36}H_{74}$, $r_0 \approx 18\mu$m, $h \approx 1\mu$m, $\Theta \approx 20°$, Simulation data: r_0/h=20, $\Theta = 15°$.

Fig. S1 shows experimental data on the melting scenario of cylinder islands of long chain alkane islands. Fig. S1a reveals how the rouloid volume increases as the temperature is

increasing slowly. Fig. S1b shows how a rouloid morphology transforms (isothermally) into a bulged morphology while the liquid volume fraction increases. The top row of fig. S1b) shows the simulation of the evolution of the surface morphology, the lower row experimental observations for similar real shapes/conditions. The simulation data are resized to the experimental scales and the red lines in the experimental data show the residual solid cylinder core from the simulated data projected on the experimental observations.

References

(S1) Pawlow, P. Über die Abhängigkeit des Schmelzpunktes von der Oberflächenenergie eines festen Körpers. *Z. Phys. Chem* **1909**, *65*, 1–35.

(S2) Takagi, M. Electron-Diffraction Study of Liquid-Solid Transition of Thin Metal Films. *J. Phys. Soc. Jpn.* **1954**, *9*, 359–363.

(S3) Buffat, P.; Borel, J. P. Size Effect on the Melting Temperature of Gold Particles. *Phys. Rev. A* **1976**, *13*, 2287–2298.

(S4) Couchman, P. R.; Jesser, W. A. Thermodynamic Theory of Size Dependence of Melting Temperature in Metals. *Nature* **1977**, *269*, 481–483.

(S5) Reiss, H.; Mirabel, P.; Whetten, R. L. Capillarity Theory for the "Coexistence" of Liquid and Solid Clusters. *J. Phys. Chem.* **1988**, *92*, 7241–7246.

(S6) Mei, Q.; Lu, K. Melting and Superheating of Crystalline Solids: From Bulk to Nanocrystals. *Prog. Mater. Sci.* **2007**, *52*, 1175–1262.

(S7) Unruh, K.; Huber, T.; Huber, C. Melting and Freezing Behavior of Indium Metal in Porous Glasses. *Phys. Rev. B* **1993**, *48*, 9021.

(S8) Herring, C. Some Theorems on the Free Energies of Crystal Surfaces. *Phys. Rev.* **1951**, *82*, 87.

(S9) Nozières, P. In *Solids Far from Equilibrium*; Godrèche, C., Ed.; Cambridge University Press Cambridge, UK, 1992; Chapter 1.